Published in final edited form as:
Radiat Phys Chem Oxf Engl 1993. 2012 January ; 81(1): 46–51. doi:10.1016/j.radphyschem.2011.09.006.

DNA Binding Hydroxyl Radical Probes

Vicky J Tang, **Katie M Konigsfeld**, **Joe A Aguilera**, and **Jamie R Milligan**
Department of Radiology, University of California at San Diego, 9500 Gilman Drive, La Jolla, CA 92093-0610

Abstract

The hydroxyl radical is the primary mediator of DNA damage by the indirect effect of ionizing radiation. It is a powerful oxidizing agent produced by the radiolysis of water and is responsible for a significant fraction of the DNA damage associated with ionizing radiation. There is therefore an interest in the development of sensitive assays for its detection. The hydroxylation of aromatic groups to produce fluorescent products has been used for this purpose. We have examined four different chromophores which produce fluorescent products when hydroxylated. Of these, the coumarin system suffers from the fewest disadvantages. We have therefore examined its behavior when linked to a cationic peptide ligand designed to bind strongly to DNA.

Keywords

ionizing radiation; DNA damage; OH radical; fluorescence

1. Introduction

Chemical modifications produced in DNA by ionizing radiation are generally held responsible for its biological effects. The two mechanisms by which these chemical modifications are introduced are the direct effect (ionization of the DNA itself) and the indirect effect (resulting from the reactive intermediates produced by the ionization of the aqueous solvent medium). The hydroxyl radical (•OH) is the species responsible for the majority of the indirect effect.

Because of its role in producing DNA damage, a variety of means have been developed for the detection of •OH in different experimental systems (Freinbichler et al. 2008). Spin traps offer the high sensitivity available with electron paramagnetic resonance detection, but they suffer from artifacts which render them unspecific (Zoia and Argyropoulos, 2010). Luminescence methods require reactive substrates (Schiller et al, 1999). Fluorescence methods are available for a range of oxidative reactive species, but these also suffer from poor specificity (Candieas at al, 1993; Wardman, 2007). However, because of the highly oxidizing nature of the hydroxyl radical, it has proved possible to devise sensitive fluorescence assays which are also highly selective for it. Examples are those based on aromatic hydroxylation (Maskos et al, 1990; Maskos et al, 1992). The hydroxyl radical will add to an aromatic ring. Electron removal from the resulting radical species forms a stable

Address for correspondence: Jamie Milligan, jmilligan@ucsd.edu, Phone 858-534-0265, Fax 858-534-0265.

hydroxylated product. Only mild oxidizing agents are required for the electron removal step. In aerobic solutions oxygen will suffice, and ferricyanide is also suitable.

The hydroxylation of benzoates to their 2-hydroxy derivatives (also called salicylates) has long found use as a dosimeter and hydroxyl radical probe (Matthews, 1980; Barreto et al, 1995; Saran and Summer, 1999). However it tends to be cumbersome to use in complex systems. The short excitation wavelengths (maximum absorption at about 300 nm) tend to overlap extensively with many biochemical species, and a chromatographic separation step is necessary (Halliwell and Kaur, 1997). Other hydroxylated aromatic systems are also fluorescent, examples being 7-hydroxycoumarin (Maeyama et al, 1992;), 7-hydroxy-2-quinolone (Lamania et al, 2010), and 7-hydroxyphenoxazin-3-one (Zhu et al, 2010). The coumarin system has found regular use as a hydroxyl radical probe (Manevich et al, 1997; Soh et al, 2008; Louit et al, 2009; Yuan et al, 2010; Page et al. 2011) or in radiation dosimetry (Collins et al, 1994; Maeyama et al, 2011), but the other systems do not appear to have been evaluated to a similar extent. There also exist other fluorescence methods which rely on different principles (Tai et al, 2002; Tachikawa and Majima, 2010).

The popularity of the coumarin system does not appear to rest on any systematic comparison with other hydroxylated aromatic fluorophores. Therefore we have compared it with the other targets mentioned above. We have also quantified its reactivity when linked to a cationic ligand designed to bind strongly to DNA.

2. Experimental section

2.1. Chemical compounds

The structures of the hydroxylated fluorescent probes and their precursors are depicted in figure 1. The names of these compounds are: 3-acetamidobenzoic acid (**1a**), 3-acetamido-5-hydroxybenzoic acid or *N*-acetylmesalazine (**1b**), 4-methylquinolin-2(1*H*)-one (**2a**), 7-hydroxy-4-methylquinolin-2(1*H*)-one (**2b**), 4-methyl-2*H*-chromen-2-one or 4-methylcoumarin (**3a**), 7-hydroxy-4-methyl-2*H*-chromen-2-one or 4-methylumbelliferone (**3b**), 7-amino-4-methyl-2*H*-chromen-2-one or 7-amino-4-methylcoumarin (**3c**), actinomycin D (**4a**), 7-hydroxyactinomycin D (**4b**), 7-aminoactinomycin D (**4c**), *N*-(coumarin-3-carboxyl)-hexa-L-arginine amide (**5a**), *N*-(7-hydroxycoumarin-3-carboxyl)-hexa-L-arginine amide (**5b**), coumarin-3-carboxylic acid (**6a**), and 7-hydroxy-coumarin-3-carboxylic acid (**6b**). The labeled peptide ligand **5a** was supplied by Biosynthesis (Lewisville, TX).

2.2. Irradiation conditions

A solution of one of the precursor compounds (1×10^{-4} mol L^{-1} **1a**, 1×10^{-4} mol L^{-1} **2a**, 1×10^{-4} mol L^{-1} **3a**, 3×10^{-6} mol L^{-1} **4a**, 3×10^{-6} mol L^{-1} **5a**, or 1×10^{-4} mol L^{-1} **5a**) was prepared in an aqueous buffer (1×10^{-2} mol L^{-1} phosphate, pH 7.0). Compounds **4a** and **5a** were used at a lower concentration because of their expense. A scavenger was also present in solution. It was either DMSO (zero to 3×10^{-4} mol L^{-1}) or glycerol (zero to 3×10^{-3} mol L^{-1}). Compound **5a** was used at two different concentrations to examine its competition with the scavenger glycerol. Aliquots (1 mL) were irradiated (1 to 250 Gy) under aerobic conditions using an AECL GammaCell-1000 instrument (JL Shepherd, San Fernando, CA) containing 400 Ci of the isotope cesium-137 (662 keV gamma ray). The dose rate of 4.6×10^{-2} Gy s^{-1} was quantified with the Fricke dosimeter (Spinks and Woods, 1990).

2.3. Fluorescence detection conditions

An aliquot (500 μL) of the irradiated solution was added to an equal volume of a solution containing sodium hydrogen carbonate (5×10^{-2} mol L^{-1}) and sodium carbonate (5×10^{-2} mol L^{-1}). The resulting solution was assayed for its fluorescence intensity and compared

with a gravimetrically calibrated solution of the corresponding authentic hydroxylated derivative. In the case of the peptide ligand **5a**, its hydroxylated derivative **5b** was not available, and 7-hydroxy-coumarin-3-carboxylic acid (**6b**) was used instead. The excitation and emission wavelengths were respectively: **1a**, 310 and 440 nm; **2a**, 350 and 435 nm; **3a**, 370 and 460 nm; **5a**, 400 and 450 nm. The intensities were recorded using a Hitachi F-7000 spectrofluorimeter (Pleasanton, CA). The instrument was calibrated with 2-aminopyridine (Lackowicz, 2006).

2.4. Behavior of 5a in the presence of plasmid DNA

All solutions contained sodium phosphate (1×10^{-2} mol L^{-1}, pH 7.0), glycerol (1×10^{-4} mol L^{-1}), the peptide ligand **5a** (2×10^{-5} mol L^{-1}), plasmid pUC18 (100 μg mL^{-1}, equivalent to 3.1×10^{-4} mol L^{-1} nucleotide residues), and spermine (zero or 5×10^{-6} to 7×10^{-4} mol L^{-1}). They were assayed in volumes of 200 μL as described below.

2.5. Pelleting

The concentrations of the plasmid and of **5a** remaining in solution after centrifugation at 12,000 × *g* for 5 min were determined from their UV absorption at 245 nm and 340 nm respectively.

2.6. Light scattering

The intensity of light scattered through a right angle was recorded using a Hitachi F-7000 spectrofluorimeter (Pleasanton, CA) with both monochromators set to a wavelength of 400 nm. This measurement was made both before and after pelleting (see above).

2.7. Strand break yield

The single strand break yield in the plasmid produced after gamma irradiation was measured using agarose gel electrophoresis. An aliquot (5 μL) of the plasmid solution was diluted with a loading buffer (15 μL) containing sucrose (15%), sodium perchlorate (1 mol L^{-1}), and bromophenol blue (0.1%). The resulting solution was loaded into the well of an agarose gel (1.2%) in the TBE buffer system and subjected to electrophoresis (1.8 V cm^{-1}) for 15 h. The fraction of the plasmid in the supercoiled form was recorded by digital video imaging of ethidium fluorescence using a GelDoc-XR instrument (Bio-Rad, Hercules, CA). The D_0 is defined as the dose required to decrease the fraction of the plasmid in the supercoiled form by a factor of *e*-fold. Assuming a Poisson distribution of DNA single strand breaks (SSBs), the D_0 dose produces a mean of one SSB per plasmid. Therefore at the D_0 dose the concentration of SSB events is equal to the concentration of the plasmid. Since the length of pUC18 is 2686 base pairs, this concentration is equal to 3.1×10^{-4} mol L^{-1} nucleotide residues, which is equivalent to $3.1\times10^{-4}/(2 \times 2686) = 5.6\times10^{-8}$ mol L^{-1} in plasmid macromolecules). The radiation chemical yield or *G*-value of SSB events is found by dividing this concentration by the value of D_0.

3. Results and discussion

3.1. Chemical structures

The structures of the target aromatic compounds (**1a**–**5a**) and their fluorescent hydroxylated derivatives (**1b**–**5b**) are depicted in figure 1. The simple coumarin derivatives (**6a** and **6b**) were employed as positive controls for the labeled peptides **5a** and **5b**. These hydroxylated derivatives are significantly more fluorescent in their deprotonated phenolate forms. In the case of 4-methylumbelliferone (**3b**) with $pK_a = 7.8$, this leads to applications as a pH indicator (Graber et al, 1986). In other cases this pH dependence is not desirable, and therefore the corresponding amino derivatives (*e.g.* **3c** and **4c**) are instead employed

(Gaforio et al, 2002; Jin et al, 2011). Naturally this is not an option when the purpose is the detection of the hydroxyl radical, and it would be necessary to increase the pH before measuring the fluorescence intensity. However, if the hydroxylated derivative is sufficiently acidic, this step would be unnecessary.

3.2. Formation of fluorescent compounds

An example of the increase in fluorescence is shown in figure 2. Irradiation of a solution of the coumarin **3a** produced a fluorescent product with excitation and emission spectra indistinguishable from those of its authentic 7-hydroxylated derivative **3b** (panel A in figure 2). Similar behavior was also observed for the benzoate **1a** and the quinolone **2a** (not shown). In the case of actinomycin D (**4a**), only a very weak fluorescence was observed and therefore this compound was not examined further. The fluorescent hydroxyl and amino derivatives of actinomycin D are known (Sengupta et al, 1978; Sengupta et al, 1981), but they appear to be formed in very low yields by ionizing irradiation. This appears reasonable given the expected extensive competition by the large cyclic peptide substitutents (Y in figure 1) and by the electron rich quinonoid ring. In the case of the coumarin labeled peptide **5a**, the authentic 7-hydroxylated derivative **5b** was not available. However, the fluorescence excitation and emission spectra observed after irradiation (panel C in figure 2) compare well with those of the structurally closely related 7-hydroxy-coumarin-3-carboxylate (panel B in figure 2) and also with those reported for a structurally very similar umbelliferone labeled polyamine (Singh et al, 2007, Singh et al, 2008). Therefore we assume that this fluorescent product is compound **5b**. In addition, we assumed that the brightness (product of the quantum yield φ and the extinction coefficient ε at the excitation maximum) of the fluorophore in **5b** is identical to that of 7-hydroxy-coumarin-3-carboxylate (Sherman and Stanfield, 1967; Adamczyk et al, 1997; Malet and Planas 1997). This value is $\varphi\times\varepsilon = 0.7 \times 3.2\times10^4$ L mol^{-1} s^{-1} = 2.2×10^4 L mol^{-1} s^{-1}.

3.3. Yields of fluorescent products

When only the fluorescent precursor is present during irradiation, essentially all of the hydroxyl radicals are available to react with it. Under these conditions, the intensity of the resulting fluorescence reflects the efficiency in which the fluorescent product is formed from the hydroxyl radical. The concentration of the fluorescent product was estimated by comparison with the fluorescence intensity of the authentic hydroxylated compound (except for **5b**, see above). From the slopes of these yield dose plots (not shown), it is possible to estimate the radiation chemical yield (or *G*-value) for the formation of the fluorescent hydroxylated products **1b**, **2b**, **3b**, and **5b** from their precursors **1a**, **2a**, **3a**, and **5a**. These yields were found to be 4.7×10^{-2} μmol J^{-1} (benzoate **1a**), 2.2×10^{-3} μmol J^{-1} (quinolone **2a**), 1.1×10^{-2} μmol J^{-1} (coumarin **3a**), and 1.4×10^{-2} μmol J^{-1} (coumarin labeled peptide **5a**). In the absence of any added scavengers, dividing this yield by that of the hydroxyl radical (equal to about 0.28 μmol J^{-1} (Pimblott and LaVerne, 1998) at the 1×10^{-4} mol L^{-1} concentration of the precursors) provides an estimate of the fraction of the hydroxyl radicals which react with the precursor that produce a fluorescent product. These yields are 17% (**1a**), 0.78% (**2a**), 3.9% (**3a**), and 5.0% (**5a**). The similarity in efficiency between **3a** and **5a** suggests a low reactivity of the hydroxyl radical with hexa-arginine in **5a**. This is consistent with the low reactivity of monomeric arginine with the hydroxyl radical (Buxton et al, 1988). The peptide groups in actinomycin D (**4a**) would be expected to be significantly more reactive towards the hydroxyl radical, since they involve the oxygen containing amino acid threonine (Buxton et al, 1988). It is also possible that the yield of 5.0% for **5b** from **5a** is a small overestimate because its brightness may differ slightly from that of **6b**.

3.4. Inhibition by scavengers

The presence during irradiation of a scavenger decreases the intensity of the resulting fluorescence. This effect is not observed if the scavenger is added after irradiation. An example is shown in figure 3, where the assumed formation of the fluorescent derivative **5b** is attenuated by the presence of glycerol during irradiation of **5a**. Similar behavior was also observed for **1a**, **2a**, and **3a** (not shown). This effect is attributed to a competition for the hydroxyl radical between the scavenger and the fluorescent precursor. If the attenuation (equivalent to the reciprocal of the *G*-value for the formation of the fluorescent product) is plotted against the concentration of the scavenger, simple competition kinetics predicts a linear relationship. Figure 4 shows that this is indeed the case for the competition between **5a** and glycerol, and that it does so at two different concentrations of **5a**. Because the rate constant for the reaction of glycerol with the hydroxyl radical is known (Buxton et al, 1988), it is possible to derive from the slopes of the lines fitted to figure 4 an estimate for the rate constant *k* between **5a** and the hydroxyl radical. For the slopes 3.72×10^{6} MJL mol^{-2} and 1.46×10^{5} MJL mol^{-2}, determined respectively at concentrations of 3×10^{-6} and 1×10^{-4} mol L^{-1} **5a**, the rate constant *k* is estimated to be 1.2×10^{10} or 9.3×10^{9} L mol^{-1} s^{-1} respectively. Similar estimates were also made for **5a** using DMSO. These were repeated for **1a**, **2a**, and **3a**. The results are listed in table 1. The agreement between rate constants estimated with two different scavengers (DMSO and glycerol) tends to support the assumption that the decrease in fluorescence is not related to quenching but instead to hydroxyl radical scavenging.

3.5. Comparison of chromophores

Although the benzoate chromophore is hydroxylated with a 17% yield to form a fluorescent product, its excitation and emission wavelengths coincide with those of DNA. This makes it awkward to use as a hydroxyl radical probe even in relatively simple cell free systems. The quinolone and phenoxazine (in the commercially available form of actinomycin D) moieties excite and emit at longer wavelengths and do not suffer from this difficulty. However, the very low yields in which they are hydroxylated make them poor choices as hydroxyl radical probes. The combination of suitable wavelengths and moderate yield for the coumarin system confirms its suitability as a hydroxyl radical probe. It has been used in this role previously, although there is little evidence for a comparison with other substrates such as we have examined here. We therefore examined the behavior of the coumarin group when linked to a cationic peptide. We found relatively little interference of the peptide with the functioning of the coumarin group in detecting hydroxyl radicals.

3.6. Application of the coumarin probe 5a

The behavior of the ligand **5a** when bound to DNA was examined using a plasmid system. We compared the SSB formation in the plasmid with the production of the fluorescent product from **5a**. To ensure that all the ligand was bound, the plasmid was present in excess. In order to produce a large change in the SSB yield we added an excess of spermine, a compound well known to aggregate DNA into particles with dimensions of hundreds of nanometers (Humpolickova et al, 2008). It has been reported that this condensation process is associated with a radioprotection against strand break formation of some two orders of magnitude (Newton et al, 1997). Aggregation of the plasmid was confirmed by both light scattering (panel A in figure 5) and pelleting (panel B in figure 5). An increase in light scattering was observed at spermine concentrations between 2×10^{-5} and 5×10^{-5} mol L^{-1}. The particles responsible for this scattering could be pelleted by a brief centrifugation. The UV absorption spectrum of the supernatant revealed that this procedure also removed the plasmid and ligand **5a** from the solution. Therefore the aggregated particles responsible for the scattering contain essentially all of the plasmid and all of **5a**.

The SSB yield recorded by the plasmid decreases extensively over the same range of spermine concentration that produces a large change in light scattering. A similar decrease can be observed in the formation of the fluorescent product from **5a**. The relative yields of these two products depend on the concentrations of the precursor, its rate constant with the hydroxyl radical, and the yield in which the detected product is formed. Representative values would be 3.1×10^{-4} mol L^{-1} nucleotide residues or 2×10^{-5} mol L^{-1} **5a** (see Experimental section); *ca*. 4×10^{8} L mol^{-1} s^{-1} for the plasmid under the poorly scavenged experimental conditions (Milligan et al, 1996) or *ca*. 1×10^{10} L mol^{-1} s^{-1} for **5a** (see table 1); and 12% for a SSB event (Milligan et al, 1993) or 5% for formation of **5b** (see above). The products of these three factors for SSB formation or for the formation of **5b** from **5a** fortuitously differ from one another by less than 2-fold. This is presumably responsible for the close agreement between the yield of SSB events and that of the formation of **5b**. Note that the absolute yields of the products also depend on the concentration of the additional scavenger glycerol, which is present at the relatively low level of 1×10^{-4} mol L^{-1}. It was added to provide a consistent scavenging capacity that would be largely unaffected by the spermine concentration.

The close correlation of the large effect of spermine on the SSB yield and on the formation of **5b** suggests that the ligand **5a** provides a reliable measurement of the accessibility of the hydroxyl radical to the environment of the DNA.

Acknowledgments

Supported by PHS grant CA46295.

References

Adamczyk M, Cornwell M, Huff J, Rege S, Rao TVS. Novel 7-hydroxycoumarin based fluorescent labels. Bioorg Med Chem Lett. 1997; 7:1985–1988.

Barreto JC, Smith GS, Strobel NH, McQuillin PA, Miller TA. Terephthalic acid: a dosimeter for the detection of hydroxyl radicals in vitro. Life Sci. 1995; 56:PL89–96. [PubMed: 7823778]

Buxton GV, Greenstock CL, Helman WP, Ross AB. Critical review of rate constants for reactions of hydrated electrons, hydrogen atoms and hydroxyl radicals in aqueous solution. J Phys Chem Ref Data. 1988; 17:513–886.

Candeias LP, Patel KB, Stratford MR, Wardman P. Free hydroxyl radicals are formed on reaction between the neutrophil-derived species superoxide anion and hypochlorous acid. FEBS Lett. 1993; 333:151–153. [PubMed: 8224156]

Collins AK, Makrigiorgos GM, Svensson GK. Coumarin chemical dosimeter for radiation therapy. Med Phys. 1994; 21:1741–1747. [PubMed: 7891636]

Freinbichler W, Bianchi L, Colivicchi MA, Ballini C, Tipton KF, Linert W, Corte LD. The detection of hydroxyl radicals in vivo. J Inorg Biochem. 2008; 102:1329–1333. [PubMed: 18262275]

Gaforio JJ, Serrano MJ, Algarra I, Ortega E, de Cienfuegos GA. Phagocytosis of apoptotic cells assessed by flow cytometry using 7-aminoactinomycin-D. Cytometry. 2002; 49:8–11. [PubMed: 12210605]

Graber ML, DiLillo DC, Friedman BL, Pastoriza-Munoz E. Characteristics of fluoroprobes for measuring intracellular pH. Anal Biochem. 1986; 156:202–212. [PubMed: 3740410]

Halliwell B, Kaur H. Hydroxylation of salicylate and phenylalanine as assays for hydroxyl radicals: a cautionary note visited for the third time. Free Radic Res. 1997; 27:239–244. [PubMed: 9350428]

Humpolickova J, Benda A, Sykora J, Machan R, Kral T, Gasinska B, Enderlein J, Hof M. Equilibrium dynamics of spermine-induced plasmid DNA condensation revealed by fluorescence lifetime correlation spectroscopy. Biophys J. 2008; 94:L17–9. [PubMed: 17965130]

Jin X, Uttamapinant C, Ting AY. Synthesis of 7-aminocoumarin by Buchwald-Hartwig cross coupling for specific protein labeling in cells. ChemBioChem. 2011; 12:65–70. [PubMed: 21154801]

Lackowicz, JR. Principles of fluorescence spectroscopy. 3. Springer; New York: 2006.

Lamania DS, Reddya KRV, Naika HSB, Paib KSR, Fasiullac RK, Naika HRP, Naikd LR. Synthesis, antitumor, and DNA binding behavior of novel 4-(2-hydroxyquinolin-3-yl)-6-phenyl-5,6-dihydropyrimidine derivatives in aqueous medium. Nucleosides Nucleotides and Nucleic Acids. 2010; 29:591–605.

Louit G, Hanedanian M, Taran F, Coffigny H, Renault JP, Pin S. Determination of hydroxyl rate constants by a high-throughput fluorimetric assay: towards a unified reactivity scale for antioxidants. Analyst. 2009; 134:250–255. [PubMed: 19173045]

Maeyama T, Yamashita S, Baldacchino G, Taguchi M, Kimura A, Murakami T, Katsumura Y, Matsui M, Shibata K, Muramatsu H, Sawada H, Nakayama M. Synthesis, Fluorescence, and Photostabilities of 3-(Perfluoroalkyl)coumarins. Chem Ber. 1992; 125:467–471.

Maeyama T, Yamashita S, Baldacchino G, Taguchi M, Kimura A, Murakami T, Katsumura Y. Production of a fluorescence probe in ion-beam radiolysis of aqueous coumarin-3-carboxylic acid solution. 1: beam quality and concentration dependences. Radiat Phys Chem. 2011; 80:535–539.

Malet C, Planas A. Mechanism of *bacillus* 1,3-1,4-β-D-glucan 4-glucanohydrolases: kinetics and pH studies with 4-methylumbelliferyl β-D-glucan oligosaccharides. Biochemistry. 1997; 36:13838–13848. [PubMed: 9374861]

Manevich Y, Held KD, Biaglow JE. Coumarin-3-carboxylic acid as a detector for hydroxyl radicals generated chemically and by gamma radiation. Radiat Res. 1997; 148:580–591. [PubMed: 9399704]

Maskos Z, Rush JD, Koppenol WH. The hydroxylation of the salicylate anion by a Fenton reaction and radiolysis: a consideration of the respective mechanisms. Free Radic Biol Med. 1990; 8:153–162. [PubMed: 2110109]

Maskos Z, Rush JD, Koppenol WH. The hydroxylation of phenylalanine and tyrosine: a comparison with salicylate and tryptophan. Arch Biochem Biophys. 1992; 296:521–529. [PubMed: 1321588]

Matthews RW. The radiation chemistry of the terephthalate dosimeter. Radiat Res. 1980; 83:27–41. [PubMed: 7394166]

Milligan JR, Aguilera JA, Ward JF. Variation of single strand break yield with scavenger concentration for plasmid DNA irradiated in aqueous solution. Radiat Res. 1993; 133:151–157. [PubMed: 8382368]

Milligan JR, Wu CCL, Ng JYY, Aguilera JA, Ward JF. Characterization of the reaction rate coefficient of DNA with the hydroxyl radical. Radiat Res. 1996; 146:510–513. [PubMed: 8896577]

Newton GL, Aguilera JA, Ward JF, Fahey RC. Effect of polyamine induced compaction and aggregation of DNA on the formation of radiation induced strand breaks: quantitative models for cellular radiation damage. Radiat Res. 1997; 148:272–284. [PubMed: 9291359]

Page SE, Wilke KT, Pierre VC. Sensitive and selective time-gated luminescence detection of production of a fluorescence probe in ion-beam radiolysis of aqueous coumarin-3-carboxylic acid solution 1. Beam quality and concentration dependences. Chem Commun. 2010; 46:2423–2425.

Pimblott SM, LaVerne JA. Effect of electron energy on the radiation chemistry of liquid water. Radiat Res. 1998; 150:159–169. [PubMed: 9692361]

Saran M, Summer KH. Assaying for hydroxyl radicals: hydroxylated terephthalate is a superior fluorescence marker than hydroxylated benzoate. Free Radic Res. 1999; 31:429–436. [PubMed: 10547187]

Schiller J, Arnhold J, Schwinn J, Sprinz H, Brede O, Arnold K. Differences in the reactivity of phthalic hydrazide and luminol with hydroxyl radicals. Free Radic Res. 1999; 30:45–57. [PubMed: 10193573]

Sengupta SK, Schaer D. The interaction of 7-substituted actinomycin D analogs with DNA. Biochim Biophys Acta. 1978; 521:89–100. [PubMed: 568940]

Sengupta SK, Anderson JE, Kogan Y, Trites DH, Beltz WR, Madhavarao MS. N2- and C-7-Substituted actinomycin D analogs: synthesis, DNA-binding affinity, and biochemical and biological properties. Structure-activity relationship. J Med Chem. 1981; 24:1052–1059. [PubMed: 6169834]

Sherman WR, Stanfield EF. Measurement of the arylsulphatase of *Patella vulgata* with 4-methylumbelliferone sulphate. Biochem J. 1967; 102:905–909. [PubMed: 16742508]

Singh A, Chen K, Adelstein SJ, Kassis AI. Synthesis of coumarin-polyamine-based molecular probe for the detection of hydroxyl radicals generated by gamma radiation. Radiat Res. 2007; 168:233–242. [PubMed: 17638412]

Singh A, Yang Y, Adelstein SJ, Kassis AI. Synthesis and application of molecular probe for detection of hydroxyl radicals produced by $Na^{125}I$ and gamma-rays in aqueous solution. Int J Radiat Biol. 2008; 84:1001–1010. [PubMed: 19061124]

Soh N, Makihara K, Ariyoshi T, Seto D, Maki T, Nakajima H, Nakano K, Imato T. Phospholipid-linked coumarin: a fluorescent probe for sensing hydroxyl radicals in lipid membranes. Anal Sci. 2008; 24:293–296. [PubMed: 18270426]

Spinks, JWT.; Woods, RJ. An introduction to radiation chemistry. 3. Wiley; New York: 1990.

Tachikawa T, Majima T. Single-molecule, single-particle fluorescence imaging of TiO_2 based photocatalytic reactions. Chem Soc Rev. 2010; 39:4802–4819. [PubMed: 20824247]

Tai C, Gu X, Zou H, Guo Q. A new simple and sensitive fluorometric method for the determination of hydroxyl radical and its application. Talanta. 2002; 58:661–667. [PubMed: 18968795]

Wardman P. Fluorescent and luminescent probes for measurement of oxidative and nitrosative species in cells and tissues: Progress, pitfalls, and prospects. Free Radical Biol Med. 2007; 43:995–1022. [PubMed: 17761297]

Yuan L, Lin W, Song J. Ratiometric fluorescent detection of intracellular hydroxyl radicals based on a hybrid coumarin-cyanine platform. Chem Commun. 2010; 46:7930–7932.

Zhu A, Romero R, Petty HR. Amplex UltraRed enhances the sensitivity of fluorimetric pyruvate detection. Anal Biochem. 2010; 403:123–125. [PubMed: 20382105]

Zoia L, Argyropoulos DS. Characterization of free radical spin adducts of the DIPPMPO using mass spectrometry and (31)P NMR. Eur J Mass Spectrom. 2010; 16:175–185.

- Examined four aromatic groups as a means to detect hydroxyl radicals by fluorescence.
- Coumarin system suffers from the fewest disadvantages.
- Characterized its reactivity when linked to a hexa-arginine peptide.

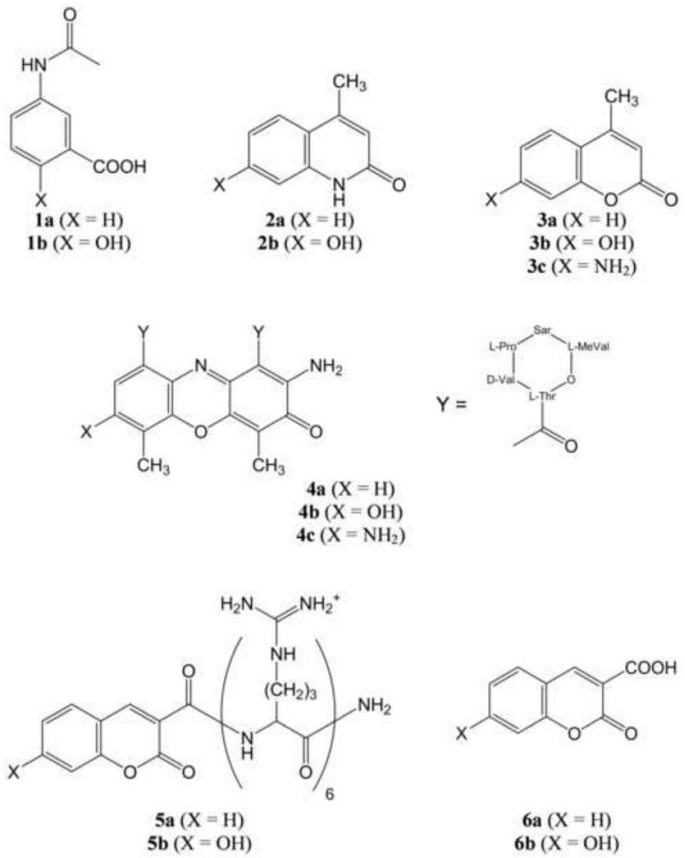

Figure 1.
Chemical structures of the compounds examined in this study.

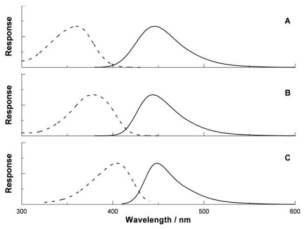

Figure 2.

Normalized fluorescence excitation (broken lines) and emission (solid lines) of **2b** (A), 7-hydroxycoumarin-3-carboxylic acid (B), and the product derived from gamma irradiation of **5a** (C), assumed to be its 7-hydroxylated derivative, **5b**. The excitation and emission maxima are located at wavelengths of 360 nm and 447 nm (panel A); 377 nm and 444 nm (panel B); and 404 nm and 448 nm (panel C). The units of the vertical scales are arbitrary.

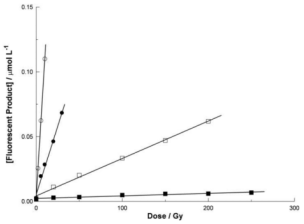

Figure 3.

Yield dose plot for the formation of the fluorescent product from **5a** (assumed to be **5b**). The hexa-arginine peptide **5a** (3×10^{-6} mol L^{-1}) was gamma irradiated in aqueous solution in the presence of glycerol at a concentration of 1×10^{-5} mol L^{-1} (open circle), 1×10^{-4} mol L^{-1} (closed circle), 1×10^{-3} mol L^{-1} (open square), or 1×10^{-2} mol L^{-1} (closed square). The concentration of the fluorescent product **5b** was estimated by assuming its brightness was identical to that of 7-hydroxy-coumarin-3-carboxylic acid (see text). The four data sets are each fitted with a least mean square straight line of the form $y = mx + c$. The values of the slopes m are 1.04×10^{-2} μmol J^{-1} (open circle), 2.04×10^{-3} μmol J^{-1} (closed circle), 2.83×10^{-4} μmol J^{-1} (open square), or 2.73×10^{-5} μmol J^{-1} (closed square).

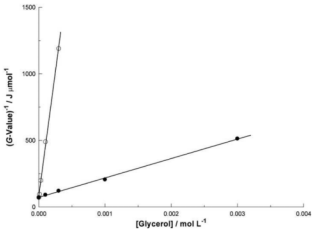

Figure 4.

Competition kinetics plot of the attenuation by glycerol of the formation of the fluorophore (assumed to be **5b**) produced by gamma irradiation of the peptide **5a** (3×10^{-6} mol L^{-1}, open circle; or 1×10^{-4} mol L^{-1}, closed circle). The two data sets are each fitted with a least mean square straight line of the form $y = mx + c$. The values of the slopes m are 3.72×10^{6} MJL mol^{-2} (open circle) or 1.46×10^{5} MJL mol^{-2} (closed circle).

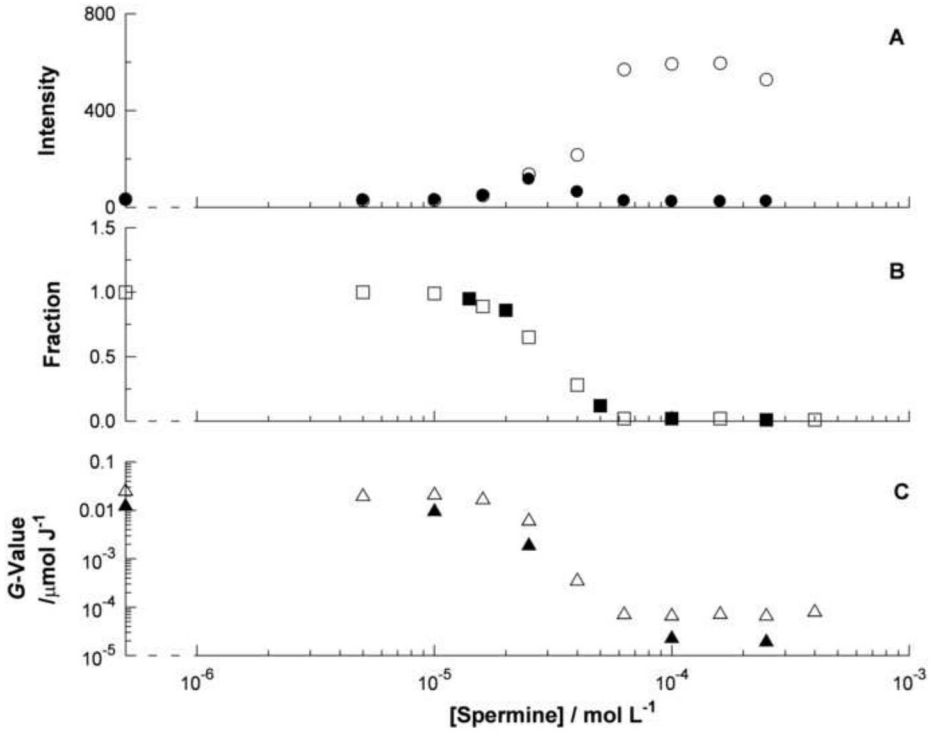

Figure 5.

Effect of spermine concentration on: the intensity of light scattering before and after centrifugation (open and closed circle symbol respectively, panel A); the fraction of the plasmid and of **5a** remaining in solution after sedimentation (open and closed square symbol respectively, panel B); the yield of strand breaks and of **5b** produced after gamma irradiation (open and closed triangle symbol respectively, panel C). The units of the vertical scale in panel A are arbitrary.

Table 1

Values of rate constants *k* for the reactions of **1a**, **2a**, **3a**, and **5a** with the hydroxyl radical.

		k/L mol^{-1} s^{-1}	
Precursor	**Structure**	**DMSO**	**Glycerol**
1a	Benzoate	5.0×10^{9}	4.3×10^{9}
2a	Quinolone	1.1×10^{10}	1.4×10^{10}
3a	Coumarin	8.7×10^{9}	8.7×10^{9}
5a	Coumarin	1.0×10^{10}	9.3×10^{9}, 1.2×10^{10}